Adsorptive Removal of Rhodamine 6G from Aqueous Solution by MMT/P (MA-co-AA) Composites: Thermodynamic study

Sajid S. Abbas[1], and Layth S. Jasim[2]
[1, 2]Department of Chemistry, College of Education, University of Al-Qadisiyah, Diwaniya, Iraq
layth.alhayder@qu.edu.iq

Abstract
Adsorption of Rhodamine 6G from Solution on montmorillonite / poly (malic acid-co-acrylic acid) Composite Surfaces is the focus of this study. Quantitative adsorption data has been obtained using the visible-spectrophotometric technique under a temperature condition. Intraparticle diffusion was found to be an important player in the desorption process based on kinetic studies. Based on the calculated data, the adsorption isotherms are classified as S-curves by Giles. The Temperature was used to study the adsorption process (15, 20, 25 and 30ºC). A decrease in the composites' ability to absorb Rhodamine 6G was found to occur with increasing temperature (exothermic process). There have also been calculations of the fundamental thermodynamic functions.
Keywords: Adsorption, Rhodamine 6G, Montmorillonite, malic acid, acrylic acid, Acrylic Acid

1. Introduction

Pharmaceutical plants, hospitals, municipal areas, and human waste [1]. Generally contain a variety of hazardous organic pollutants that are rarely biodegradable, even at low concentrations [2, 3] . The introduction of new pollutants into the environment harms ecological species and constitutes a serious threat to human and aquatic health [4, 5]. Separation of solid phases [6] For the absorption of pharmaceutical-laden wastewater, flocculation, coagulation[7], ultrasonic degradation[8], photodegradation[9], electrochemical degradation[10], and advanced oxidation procedures have all been explored[11].These technologies have a lot of flaws since they are either technologically sophisticated or economically unfavorable. In addition, they emit toxic waste and have a low removal effectiveness[12]. When it comes to dealing with effluents, adsorption is a preferred option. Adsorption is a popular method for treating effluents because of its simplicity, economic feasibility, lack of secondary products and free radicals, broad surface area, and presence of functional groups with established pore assembly[13]. Olive stone activated carbon, vine wood[14], Guava seeds, Moringa oleifera[15], Pine tree and Mn-impregnated activated carbon are some of the plants used in this study. guava seeds, Moringa oleifera[16], pine tree, and Mn-impregnated activated carbon are examples of carbon-based sorbents[17].

Due to the combining characteristics of both clays and polymers, such as biodegradability, biocompatibility, economic viability, abundance, high specific surface area, three-dimensional network, and swelling–deswelling properties, clay-based hydrogel nanocomposites are envisioned to be potential super adsorbents for the uptake of inorganic and/or organic contaminants from a Clay-based hydrogel nanocomposites are envisioned to be potential super adsorbents for the. Hydrogels are a form of polymer that does not dissolve in water at physiological temperatures or pH values, but expands dramatically when exposed to water [18-20].

These are three-dimensional crosslinked polymeric materials with the ability to absorb and retain a large amount of water, making them suitable for a variety of bioengineering, biomedical, food, and pharmaceutical applications [21, 22].

Water insoluble properties are assumed to be caused by the presence of chemical or physical cross-links, which provide the system with integrity and physical stability. Water can infiltrate through the network structure of hydrogels because of their porosity, which is governed by a number of factors such as the polymer's chemical composition, hydrophilicity, and chemical structure, as well as cross-link density and cross-linker activity[23]. The existence of chemical or physical cross-links, which Many clay-based hydrogel hybrids have recently been explored for the absorption of dyes because of their chemically reactive functional groups and porous topologies, provide the system with as well as metals [24, 25]. According to a literature review, little work has been done The major purpose was to assess the performance of a poly(acrylic acid-maleic acid)/montmorillonite hydrogel nanocomposite for the removal of pharmaceutical contaminants via clay–hydrogel nanocomposites. Rohdamen 6G uptake from wastewater. As a filler, nanoscale MMT was used, The mechanical strength, active spots for maximal sorption, a high surface area, and improved regenerative mechanical strength All of nanocomposite's abilities could be upgraded. The capacity for adsorption has increased. From a practical standpoint, reusability is essential. To further understand the adsorption mechanism and the effects of operative parameters such pH, and strength, active research is being conducted. The initial sorbate level was investigated. To further understand the processability of nanocomposite, equilibrium data was analyzed using

doi.org/10.31838/hiv22.02.222 Received: 29.06.22, Revised: 30.06.22, Accepted: 25.08.22

various kinetic and isotherm models, as well as thermodynamic characteristics.

2. Materials and Procedures

Instruments

Sartorius Lab. L420 B, +0.0001, Visible-visible spectrophotometer shimadzu 1800 PC, shaking Incubator precision Scientific, Hettich Universal (D-7200), and centrifuge tubes.

Materials

Fluka (Germany) contributed Rhodamine B (Figure 1), sodium hydroxide, sodium chloride, Montmorillonite K-10, Acrylic acid (AAc), and Maleic acid (MAc) (Himedia, India). N,N'-Methylene-bis-acrylamide (MBA) was purchased as the cross linker (Sigma-Aldrich, Germany). The firm supplied KPS, a critical component of the reaction (mercy, Germany).

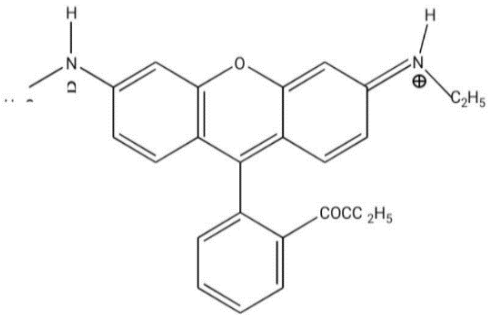

Fig. (1): Rhodamine 6G Molecular Structure

MMT/ (MA/AA) composite preparation.

In a 200 mL flask, the surface was produced by dissolving 8 mL of acrylic acid (AA) in 10 mL of deionized water and stirring continuously for 10 minutes. After 10 minutes of continuous stirring, add it to a solution (1 g in 2 mL) of malic acid (MA), then add 1.5 g of montmorillonite clay (MMT) dissolved in 2 ml of distilled water with continuous stirring for 30 minutes, then dissolve 0.08 g of MBA in 5 ml of distilled water with continuous stirring, interspersed with (N2), then add it to the above total solution with continuous stirring for 15 minutes.

With constant stirring, we dissolve 0.06 g potassium sulfate (KPS) in 5 ml distilled water. It is pumped with nitrogen gas. It is stirred continuously for 15 minutes after being added to the prior entire solution. After that, the complete solution is transferred to closed tubes, incubated for 2 hours in a water bath at 60°C. In the water bath, the temperature is raised to 70 °C and left for two hours (Figure (2).

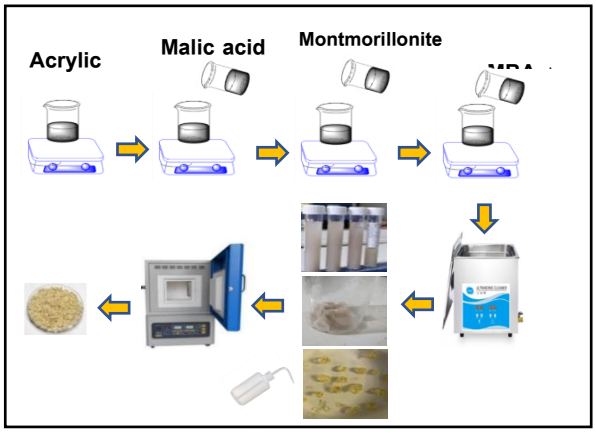

Fig. 2: Schematic diagram of stag of the MMT/ P(MA-CO-AA) composite preparation

0.05 g of composites were shaken into dye solutions with concentrations ranging from 1 to 10 mg/mL to evaluate the adsorption isotherms (1-20 ppm). After 30 minutes of shaking, the suspensions were centrifuged at 3000 rpm for 10 minutes. The dye concentration was determined using the spectrophotometric technique. The amount of Rhodamine 6G adsorbed was determined using the following formula:

$$Qe = \frac{v(c_\circ - c_e)}{m} \quad (1)$$

Where Qe is the amount adsorbed, m is the adsorbent's weight in grams (g), V is the volume of the solution in liters (L), and Co and Ce are the starting and equilibrium concentrations in milligrams per liter (mg/L).

Effect of Temperature

The adsorption experiment was repeated at temperatures ranging from 15 to 30ºC.

3. Results and Discussion

FTIR

Before and after the dye surface adsorption process, the composite was characterized using FTIR (Figure (3). The adsorption of MMT/P(MA-co-AA) composite is obviously and significantly higher. 4

MMT/ P(MA-co-AA) composite is not the same as MMT/ P(MA-co-AA) composite. In the FT-IR spectra, the intensity of bands adjacent to the adsorption decreases noticeably in the pre-adsorption composite. The adsorption process is weak due to the dye's chemical composition and acidic nature. Variations in absorption intensity are also caused by acidic particles on the surface[26].

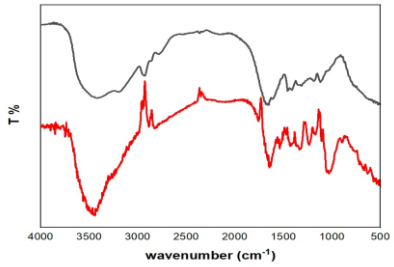

Fig. 3: FT-IR spectra of MMT/ P(MA-co-AA) composite: (a) before, (b) after adsorption of Rhodamine 6G

FESEM

The FESEM approach is used to investigate the physical

characteristics, porosity, and nature of the prepared surface, as well as the shape and size of the particles and how they are dispersed on the surface, before and after the adsorption process for each (P(MA-co-AA) composite[27]. The hydrogel surface was discovered to have many and heterogeneous pores. The surface became less rough after graphene oxide was added. Because of the graphite oxide loading, several cavities were minimized, confirming the efficacy of the adsorption procedure as shown in Figure (4).

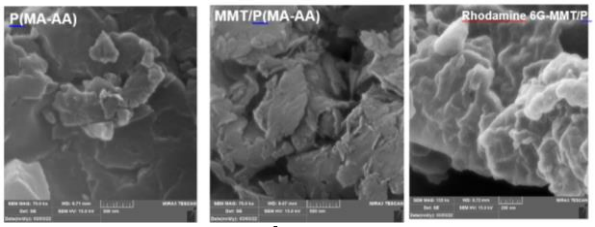

Fig. 4: FE-SEM image of P(MA-AA), MMT/ P(MA-CO-AA) composite and Rhodamine 6G-MMT/P(MA-AA)

Isotherm of Adsorption

The equilibrium isotherm was utilized to determines the Rhodamine 6G adsorption capability of composites. Figure 3 depicts the composites' equilibrium concentrations as a function of adsorption quantities. at 25°C, a dye adsorption isotherm

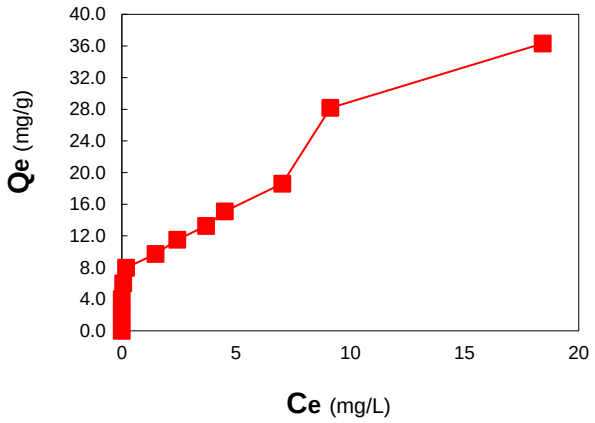

Fig. 5: Adsorption isotherm of Rhodamine 6G on composites at constant temperature (25°C)

The adsorptive capabilities of the composites improved as the Rhodamine 6G concentration increased. The specific surface area, extensibility, mobility of dye molecules in the liquid phase and in the interior of the solid, and the forces of attraction between the surface of the solid and the dye molecules are all factors that influence adsorption capacity. Coulombic forces are the most important interactions that effect dye adsorption on cellulose. The Rhodamine 6G adsorption patterns described by Giles and coworkers were found to fit S-type isotherms. It's most likely due to electrostatic adsorption of one layer followed by van der Waals attraction for the other layer, according to the form of the isotherm. the second layer's adsorption The S-type isotherm is based on the heterogeneous surface assumption of Freundlich. A variety of adsorption patterns are created by different planes, such as fibers[29 ,28]. The Langmuir, Freundlich, and Temkin equations have been solved in their linear form. The linearized Freundlich model was used to predict the adsorption of Rhodamine 6G on composites, as illustrated in Figure (4). The following is the relationship between the adsorbent's dye absorption capacity, Qe (mg/g), and the residual dye concentration at equilibrium, Ce (mg/l):

$ln\ Qe = lnk + \frac{1}{n} lnCe$ (2) where n and k are constants for the specific adsorbent and solute, respectively.

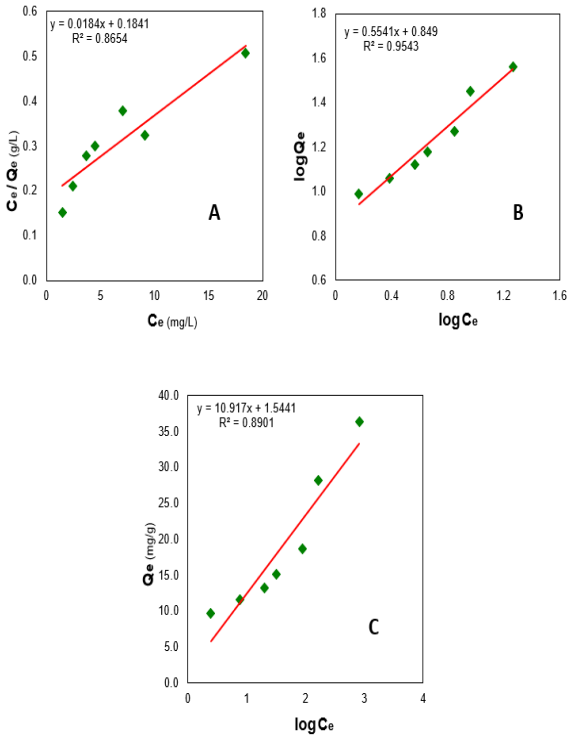

Fig. 6: (A)Langmuir, (B) Freundlich, and (C) Temkin isotherms of Rhodamine 6G on composites at constant temperature (25oC)

The isotherm fails to account for both tiny and large concentrations. It believes that covering the layer will reduce the adsorption heat of all the molecules in the layer linearly rather than logarithmically. The Langmuir, Freundlich, and Timken models were utilized to match the dye- composites method's experimental equilibrium data to the model. Figure 9 shows that the model Freundlich has the best correlation coefficients (R2= 0.9543).

Table 1: All three models of adsorption of Chromium Ion on P(CH /AA-co-AM) at 25oC: Langmuir, Fiendish and Timken

Langmuir equation			Freundlich equation			Temkin equation		
K L	R^2	qm	n	KF	R^2	KT	B	R^2
0.099	0.8654	54.3478	1.8047	7.063	0.9543	1.1511	10.917	0.8901

Figure (8) shows the general shapes of Rhodamine 6G adsorption isotherms at three different temperatures.

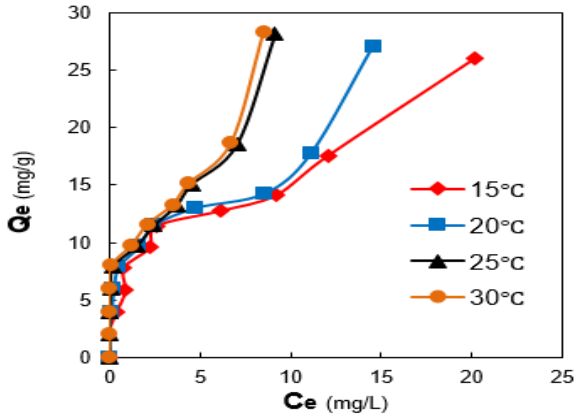

Fig. 8: Adsorption isotherms of Rhodamine 6G on composites at different temperatures

The results showed that the amount of dye that was absorbed into the composite increased slightly as the temperature rose. This made the adsorption process look like it was endothermic. Some dyes were found to be more likely to be absorbed when the temperature rose. This means that in order for the composite and the dye molecules to interact, they need a lot of energy to do so. Endothermic dye uptake can also be linked to the possibility of a dye being absorbed or absorbed by the surface. The solvent may make the composite swell so much that both the solvent and the dye can get the job done. We looked at Xm values at different temperatures to figure out the basic thermodynamic quantities of Rhodamine 6G adsorption on composite. You can figure out how much heat is absorbed if you know Van't Hoff's equation (eq. (3)[30-32].

$$\ln X_m = \frac{-\Delta H}{RT} + \text{constant} \quad (3)$$

Table (2) and Figure (9) demonstrate these calculations.

Table (2): The effect of temperature on the maximum amount of Rhodamine 6G that can be adsorb onto composite

T(K)	1000/T(K-1)	Ce	Xm	$\ln Xm$
288	3.4722	3.2	11.9	2.4765
293	3.4129	3.2	12.2	2.5014
298	3.3557	3.2	12.6	2.5336
303	3.3003	3.2	12.9	2.5572

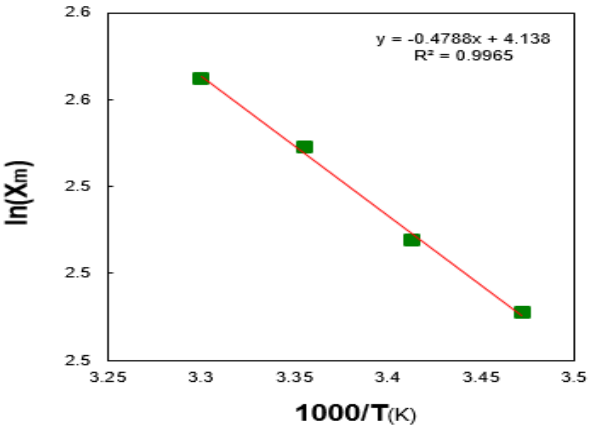

Fig. 10: Plot of ln Xm vs. 1000/T of adsorption of Rhodamine 6G onto composite

The change in free energy (ΔG) and the change in entropy (ΔS) could be found from the equation (4) and (&) and (5):

$$\Delta G = -RT ln\, K_{eq} \quad (4)$$

$$\Delta G = \Delta H - T.\Delta S \quad (5)$$

Table (3) shows the basic thermodynamic values of the adsorption of crystal violet on the composite shown in the table. Values show that an adsorption of the van der Waals type is likely to happen[33-36]

Table (3): Rhodamine 6G adsorption onto a surface due to thermodynamic factors

ΔG KJ/mol	ΔH KJ/mol	ΔS J. K^{-1}. mol^{-1}	Equilibrium (k)
-5.027	3.980	30.227	3.15

Effect of pH on the Adsorption

By controlling various temperature and time variables, the influence of the pH function on the adsorption of rhodamine 6G dye at a concentration of (200 ppm) on the adsorbent surface of the MMT/P(MA-co-AA) compound at varied pH values (2-10) was investigated. The findings revealed that the acidity function has an impact on the adsorbent material and the adsorbing surface, as well as the interactions between them. The amount of adsorption on the adsorbent surface increases as the acidic function increases, which is owing to the fact that when the pH is low, the concentration of H+ is low. There will be a competitive competition between them if the concentration of ions in the solution is quite high. And between the dye molecules on the active sites of the adsorbent surface that have a positive charge, which lowers adsorption.

When the pH is raised, the carboxyl and hydroxyl groups on the adsorbing surface ionize and lose a proton, resulting in a negatively charged adsorbing surface. Electrostatic attraction then occurs between the positively charged dye molecules and the adsorbing surface, resulting in an increase in adsorption as the function is increased. Acidic, and there will be repulsion between the negatively charged functional groups on the adsorbent surface, causing swelling and expansion, allowing the dye molecules to diffuse within the overlaid surface, and the adsorption will increase[37, 38].

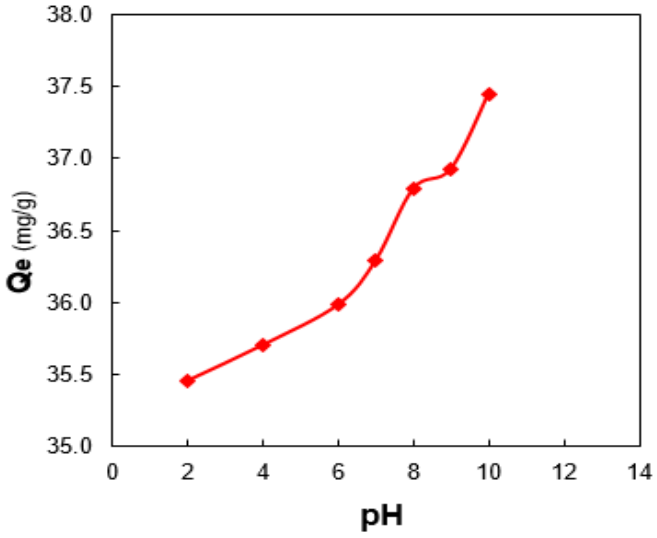

4. Conclusions

1 .The composites might be employed to extract the Rhodamine 6G dye from wastewater as an adsorbent.

2 .The amount of Rhodamine 6G adsorbed was proportional to the dye concentration.

3 .You can use Freundlich's equation to see how well the adsorption model matches.
4 .The Freundlich isotherm was followed by Rhodamine 6G adsorption isotherms on composites.
5. Thermodynamic parameters show that the adsorption process is endothermic and spontaneous, suggesting that as the temperature rises, sorption will increase.

Reference

1. Chen C, Wang P, Lim T-T, Liu L, Liu S, Xu R. A facile synthesis of monodispersed hierarchical layered double hydroxide on silica spheres for efficient removal of pharmaceuticals from water. Journal of Materials Chemistry A. 2013;1(12):3877-80. Available from: https://pubs.rsc.org/en/content/articlelanding/2013/ta/c3ta10197e/unauth
2. Kolpin DW, Furlong ET, Meyer MT, Thurman EM, Zaugg SD, Barber LB, Buxton HT. Pharmaceuticals, hormones, and other organic wastewater contaminants in US streams, 1999− 2000: A national reconnaissance. Environmental science & technology. 2002;36(6):1202-11. https://doi.org/10.1021/es011055j
3. Abdulsahib WK, Sahib HH, Mahdi MA, Jasim LS. Adsorption study of cephalexin monohydrate drug in solution on poly (vinyl pyrrolidone-acryl amide) hydrogel surface. Int J Drug Deliv Technol. 2021;11(4):1169-72. Available from: http://impactfactor.org/PDF/IJDDT/11/IJDDT,Vol11,Issue4,Article9.pdf
4. Ganduh SH, Aljeboree AM, Mahdi MA, Jasim LS. Spectrophotometric Determination of Metoclopramide-HCl in the standard raw and it compared with pharmaceuticals. Journal of Pharmaceutical Negative Results. 2021;12(2):44-8. Available from: https://www.researchgate.net/publication/358854079
5. Zhang Y, Habteselassie MY, Resurreccion EP, Mantripragada V, Peng S, Bauer S, Colosi LM. Evaluating removal of steroid estrogens by a model alga as a possible sustainability benefit of hypothetical integrated algae cultivation and wastewater treatment systems. ACS Sustainable Chemistry & Engineering. 2014;2(11):2544-53. https://doi.org/10.1021/sc5004538
6. Evans SE, Davies P, Lubben A, Kasprzyk-Hordern B. Determination of chiral pharmaceuticals and illicit drugs in wastewater and sludge using microwave assisted extraction, solid-phase extraction and chiral liquid chromatography coupled with tandem mass spectrometry. Analytica chimica acta. 2015;882:112-26.
7. Mir-Tutusaus JA, Parladé E, Llorca M, Villagrasa M, Barceló D, Rodriguez-Mozaz S, Martinez-Alonso M, Gaju N, Caminal G, Sarrà M. Pharmaceuticals removal and microbial community assessment in a continuous fungal treatment of non-sterile real hospital wastewater after a coagulation-flocculation pretreatment. Water research. 2017;116:65-75.
8. Hassan H, Almarjeh RAB, Atassi Y. In-Vitro Ibuprofen Release Monitoring Using Carbon Quantum Dots. Journal of Fluorescence. 2021;31(1):289-303. https://doi.org/10.1007/s10895-020-02659-z
9. Khorasanizadeh MH, Hajizadeh-Oghaz M, Khoobi A, Ganduh SH, Mahdi MA, Abdulsahib WK, Jasim LS, Salavati-Niasari M. Synthesis and characterization of HoVO4/CuO nanocomposites for photodegradation of methyl violet. International Journal of Hydrogen Energy. 2022;47(46):20112-28. https://doi.org/10.1016/j.ijhydene.2022.04.136. Available from: https://www.sciencedirect.com/science/article/pii/S0360319922017062
10. Liu X, Yang D, Zhou Y, Zhang J, Luo L, Meng S, Chen S, Tan M, Li Z, Tang L. Electrocatalytic properties of N-doped graphite felt in electro-Fenton process and degradation mechanism of levofloxacin. Chemosphere. 2017;182:306-15. https://doi.org/10.1016/j.chemosphere.2017.05.035
11. Isarain-Chávez E, Rodríguez RM, Cabot PL, Centellas F, Arias C, Garrido JA, Brillas E. Degradation of pharmaceutical beta-blockers by electrochemical advanced oxidation processes using a flow plant with a solar compound parabolic collector. Water research. 2011;45(14):4119-30. https://doi.org/10.1016/j.watres.2011.05.026
12. Mudassir MA, Hussain SZ, Jilani A, Zhang H, Ansari TM, Hussain I. Magnetic hierarchically macroporous emulsion-templated poly (acrylic acid)–iron oxide nanocomposite beads for water remediation. Langmuir. 2019;35(27):8996-9003. https://doi.org/10.1021/acs.langmuir.9b01121
13. Khan EA, Khan TA. Adsorption of methyl red on activated carbon derived from custard apple (Annona squamosa) fruit shell: equilibrium isotherm and kinetic studies. Journal of Molecular Liquids. 2018;249:1195-211. https://doi.org/10.1016/j.molliq.2017.11.125
14. Berbar Y, Hammache ZE, Bensaadi S, Soukeur R, Amara M, Van der Bruggen B. Effect of functionalized silica nanoparticles on sulfonated polyethersulfone ion exchange membrane for removal of lead and cadmium ions from aqueous solutions. Journal of Water Process Engineering. 2019;32:100953. https://doi.org/10.1016/j.jwpe.2019.100953
15. Cazetta AL, Vargas AMM, Nogami EM, Kunita MH, Guilherme MR, Martins AC, Silva TL, Moraes JCG, Almeida VC. NaOH-activated carbon of high surface area produced from coconut shell: Kinetics and equilibrium studies from the methylene blue adsorption. Chemical Engineering Journal. 2011;174(1):117-25.
16. Viotti PV, Moreira WM, dos Santos OAA, Bergamasco R, Vieira AMS, Vieira MF. Diclofenac removal from water by adsorption on Moringa oleifera pods and activated carbon: Mechanism, kinetic and equilibrium study. Journal of Cleaner Production. 2019;219:809-17. https://doi.org/10.1016/j.jclepro.2019.02.129
17. Liu H, Hu Z, Liu H, Xie H, Lu S, Wang Q, Zhang J. Adsorption of amoxicillin by Mn-impregnated activated carbons: performance and mechanisms. RSC advances. 2016;6(14):11454-60. https://doi.org/10.1039/C5RA23256B
18. Peng N, Hu D, Zeng J, Li Y, Liang L, Chang C. Superabsorbent cellulose–clay nanocomposite hydrogels for highly efficient removal of dye in water. ACS Sustainable Chemistry & Engineering. 2016;4(12):7217-24. https://doi.org/10.1021/acssuschemeng.6b02178

19. Kim SJ, Park SJ, Kim SI. Properties of smart hydrogels composed of polyacrylic acid/poly (vinyl sulfonic acid) responsive to external stimuli. Smart Materials and Structures. 2004;13(2):317.
20. Kianipour S, Razavi FS, Hajizadeh-Oghaz M, Abdulsahib WK, Mahdi MA, Jasim LS, Salavati-Niasari M. The synthesis of the P/N-type NdCoO3/g-C3N4 nano-heterojunction as a high-performance photocatalyst for the enhanced photocatalytic degradation of pollutants under visible-light irradiation. Arabian Journal of Chemistry. 2022;15(6):103840. https://doi.org/10.1016/j.arabjc.2022.103840. Available from: https://www.sciencedirect.com/science/article/pii/S1878535222001563
21. Catoira MC, Fusaro L, Di Francesco D, Ramella M, Boccafoschi F. Overview of natural hydrogels for regenerative medicine applications. Journal of Materials Science: Materials in Medicine. 2019;30(10):1-10. https://doi.org/10.1007/s10856-019-6318-7
22. Sharma G, Thakur B, Naushad M, Kumar A, Stadler FJ, Alfadul SM, Mola GT. Applications of nanocomposite hydrogels for biomedical engineering and environmental protection. Environmental chemistry letters. 2018;16(1):113-46.
23. Kabir SM, Sikdar PP, Haque B, Bhuiyan MA, Ali A, Islam MN. Cellulose-based hydrogel materials: Chemistry, properties and their prospective applications. Progress in biomaterials. 2018;7(3):153-74.
24. Gyles DA, Castro LD, Silva Jr JOC, Ribeiro-Costa RM. A review of the designs and prominent biomedical advances of natural and synthetic hydrogel formulations. European Polymer Journal. 2017;88:373-92. https://doi.org/10.1016/j.eurpolymj.2017.01.027
25. Guo Q. Thermosets: structure, properties, and applications. Woodhead Publishing, 2017.
26. Bhagavatheswaran ES, Das A, Rastin H, Saeidi H, Jafari SH, Vahabi H, Najafi F, Khonakdar HA, Formela K, Jouyandeh M. The taste of waste: the edge of eggshell over calcium carbonate in acrylonitrile butadiene rubber. Journal of Polymers and the Environment. 2019;27(11):2478-89.
27. Zhang W, Zhang H, Yang Y, Tang P. Poly (maleic acid-co-acrylic acid) ionomer as nucleating agent on the crystallization behavior and properties of poly (ethylene terephthalate). Polymer Bulletin. 2022;79(6):3803-27.
28. Bhullar N, Kumari K, Sud D. A biopolymer-based composite hydrogel for rhodamine 6G dye removal: its synthesis, adsorption isotherms and kinetics. Iranian Polymer Journal. 2018;27(7):527-35. https://doi.org/10.1007/s13726-018-0630-9
29. Du J, Yang X, Xiong H, Dong Z, Wang Z, Chen Z, Zhao L. Ultrahigh adsorption capacity of acrylic acid-grafted xanthan gum hydrogels for rhodamine B from aqueous solution. Journal of Chemical & Engineering Data. 2021;66(3):1264-72. https://doi.org/10.1021/acs.jced.0c00850
30. Akperov OH, Kamranzadeh FM, Akperov EO. REMOVAL OF RHODAMINE 6G DYE FROM WATER SOLUTION BY ALT-MALEIC ANHYDRIDE-STYRENE COPOLYMER, CROSS-LINKED WITH HEXAMETHYLENEDIAMINE. Kimya Problemleri. 2021(4):203-14.
31. Samaddar P, Kumar S, Kim K-H. Polymer hydrogels and their applications toward sorptive removal of potential aqueous pollutants. Polymer Reviews. 2019;59(3):418-64. https://doi.org/10.1080/15583724.2018.1548477
32. Thakur S, Arotiba OA. Synthesis, swelling and adsorption studies of a pH-responsive sodium alginate–poly (acrylic acid) superabsorbent hydrogel. Polymer bulletin. 2018;75(10):4587-606.
33. Gao Z, Liu N, Wu D, Tao W, Xu F, Jiang K. Graphene–CdS composite, synthesis and enhanced photocatalytic activity. Applied Surface Science. 2012;258(7):2473-8. https://doi.org/10.1016/j.apsusc.2011.10.075
34. Prakash V, Bhar R, Sharma S, Mehta SK. Photophysical deactivation behaviour of Rhodamine B using different graphite materials. Rsc Advances. 2019;9(39):22320-6.
35. Attallah MF, Allan KF, Mahmoud MR. Synthesis of poly (acrylic acid–maleic acid) SiO2/Al2O3 as novel composite material for cesium removal from acidic solutions. J Radioanal Nucl Chem. 2016;307(2):1231-41.
36. Pathania D, Sharma A. Microwave induced graft copolymerization of binary monomers onto luffa cylindrica fiber: removal of congo red. Procedia engineering. 2017;200:408-15. https://doi.org/10.1016/j.proeng.2017.07.057
37. Moreno-Villoslada I, Fuenzalida JP, Tripailaf G, Araya-Hermosilla R, Pizarro GdC, Marambio OG, Nishide H. Comparative Study of the Self-Aggregation of Rhodamine 6G in the Presence of Poly (sodium 4-styrenesulfonate), Poly (N-phenylmaleimide-co-acrylic acid), Poly (styrene-alt-maleic acid), and Poly (sodium acrylate). The Journal of Physical Chemistry B. 2010;114(37):11983-92.
38. Fradj AB, Lafi R, Hamouda SB, Gzara L, Hamzaoui AH, Hafiane A. Effect of chemical parameters on the interaction between cationic dyes and poly (acrylic acid). Journal of Photochemistry and Photobiology A: Chemistry. 2014;284:49-54. https://doi.org/10.1016/j.jphotochem.2014.04.003